INFECTION AND IMMUNITY, Nov. 2010, p. 4511–4522 Vol. 78, No. 11
0019-9567/10/$12.00 doi:10.1128/IAI.00428-10

Translocation of *Pseudomonas aeruginosa* from the Intestinal Tract Is Mediated by the Binding of ExoS to an Na,K-ATPase Regulator, FXYD3[▽]

Jun Okuda,[1] Naoki Hayashi,[1] Masashi Okamoto,[1] Shinji Sawada,[1] Shu Minagawa,[1] Yoshitaka Yano,[2] and Naomasa Gotoh[1]*

Department of Microbiology and Infection Control Science,[1] and Educational and Research Center for Clinical Pharmacy,[2] Kyoto Pharmaceutical University, Yamashina, Kyoto 607-8414, Japan

Received 26 April 2010/Returned for modification 19 May 2010/Accepted 11 August 2010

The intestinal tract is considered the most important reservoir of *Pseudomonas aeruginosa* in intensive care units (ICUs). Gut colonization by *P. aeruginosa* underlies the development of invasive infections such as gut-derived sepsis. Intestinal colonization by *P. aeruginosa* is associated with higher ICU mortality rates. The translocation of endogenous *P. aeruginosa* from the colonized intestinal tract is an important pathogenic phenomenon. Here we identify bacterial and host proteins associated with bacterial penetration through the intestinal epithelial barrier. We first show by comparative genomic hybridization analysis that the *exoS* gene, encoding the type III effector protein, ExoS, was specifically detected in a clinical isolate that showed higher virulence in silkworms following midgut injection. We further show using a silkworm oral infection model that *exoS* is required both for virulence and for bacterial translocation from the midgut to the hemolymph. Using a bacterial two-hybrid screen, we show that the mammalian factor FXYD3, which colocalizes with and regulates the function of Na,K-ATPase, directly binds ExoS. A pulldown assay revealed that ExoS binds to the transmembrane domain of FXYD3, which also interacts with Na,K-ATPase. Na,K-ATPase controls the structure and barrier function of tight junctions in epithelial cells. Collectively, our results suggest that ExoS facilitates *P. aeruginosa* penetration through the intestinal epithelial barrier by binding to FXYD3 and thereby impairing the defense function of tight junctions against bacterial penetration.

Pseudomonas aeruginosa is an opportunistic pathogen that is a major cause of infection-related mortality among individuals with compromised immune systems. Fatality rates among patients infected with *P. aeruginosa* are higher than those among patients infected with any other opportunistic Gram-negative bacterium (48, 51). The lungs are a major site of *P. aeruginosa* infection in ill patients; however, a considerable number of such infections occur through direct contamination of the lungs by gastrointestinal flora or through hematogenous spread from the intestine to the lungs (51). In particular, the presence of highly virulent strains of *P. aeruginosa* within the intestinal tract alone is the main source of sepsis and death among immunocompromised patients, even in the absence of established extraintestinal infection and bacteremia (34, 41, 51). Furthermore, the lethal effects of intestinal *P. aeruginosa* are dependent upon its ability to adhere to and disrupt the intestinal epithelial barrier (1).

The intestinal tract is considered to be the most important reservoir of *P. aeruginosa* (2). The rate of mortality of patients in intensive care units (ICUs) suffering from intestinal colonization by *P. aeruginosa* is significantly higher than that of patients without such colonization (34). The notion that gut colonization by *P. aeruginosa* sets the stage for the underlying development of invasive infection is supported by reports demonstrating a reduction in rates of ICU-acquired infection owing to a decontamination of the digestive tract (5, 31, 46). Recently, the importance of intestinal *P. aeruginosa* as a cause of mortality in critically ill patients was demonstrated in a randomized prospective study (11). Patients were subjected to selective antibiotic decontamination of the digestive tract through the oral administration of nonabsorbable antibiotics. This resulted in decreased mortality and was associated with a decrease in fecal *P. aeruginosa*. The translocation of *P. aeruginosa* from the colonized intestinal tract, a process whereby endogenous intestinal *P. aeruginosa* relocates extraluminally, is considered an important pathogenic phenomenon.

The importance of the translocation of *P. aeruginosa* from the colonized intestinal tract in causing gut-derived septicemia was determined by exploiting leukopenic mice (35, 38, 48). In addition, most clinical blood isolates, but not human respiratory isolates, have been shown to cause lethal endogenous bacteremia in leukopenic mice (15, 24). Cytokines such as tumor necrosis factor alpha (TNF-α) and interleukin-1α have been implicated in the translocation of *P. aeruginosa* in gut-derived sepsis of leukopenic mice (36, 37). Furthermore, multidrug efflux systems of *P. aeruginosa*, such as *mexAB-oprM*, have been reported to play a key role not only in the invasiveness of the bacteria into or transmigration of the bacterium across Madin-Darby canine kidney (MDCK) cells but also in the ability of the bacteria to kill leukopenic mice (24). However, it is still unclear at the molecular level how *P. aeruginosa* exploits multidrug efflux systems to penetrate the epithelial cell barrier.

* Corresponding author. Mailing address: Department of Microbiology and Infection Control Science, Kyoto Pharmaceutical University, Misasagi-Nakauchicho 5, Yamashina, Kyoto 607-8414, Japan. Phone: 81-75-595-4641. Fax: 81-75-595-4755. E-mail: ngotoh@mb.kyoto-phu.ac.jp.

▽ Published ahead of print on 30 August 2010.

P. aeruginosa uses a type III secretion apparatus to inject effectors into host cells. The *P. aeruginosa* type III secretion system seems to have fewer effectors than any other bacterial type III secretion system: only four effector proteins, ExoS, ExoT, ExoU, and ExoY, of the *P. aeruginosa* type III secretion system have been identified. ExoS is a bifunctional toxin possessing an N-terminal Rho GTPase-activating protein (RhoGAP) activity that targets small GTPases (18, 20, 22, 49) and a highly promiscuous C-terminally encoded ADP-ribosylation activity (ADPRT) toward small GTP-binding proteins (8, 9, 20, 23). The RhoGAP activity of ExoS causes the disruption of the host cell actin cytoskeleton through modulating the switch between an active GTP-bound form and an inactive GDP-bound form. The ADPRT activity of ExoS has several effects on the host cell, such as a disruption of the actin cytoskeleton, inhibition of DNA synthesis, and cell death. The eukaryotic cofactor 14-3-3 is required for the activation of the ADPRT activity of ExoS (20). ExoT is closely related to ExoS and is also a bifunctional toxin with N-terminal GAP activity and C-terminal ADPRT activity (20). ExoU is a potent necrotizing toxin with phospholipase activity that is able to cause rapid cell death in eukaryotic cells (20). ExoY is an adenylate cyclase, and the injection of ExoY into mammalian cells causes an elevation of intracellular cyclic AMP (cAMP) levels, although the significance of ExoY in infection remains unclear (20). Recently, it was reported that infection of polarized airway epithelial cells with *P. aeruginosa* expressing type III effectors (ExoS, ExoT, and ExoY) disrupts intact tight junctions (TJs) by altering the distribution of the TJ proteins ZO-1 and occludin (44). However, the precise molecular mechanism by which the type III effector induces the disruption of TJs remains unknown. Although many binding partners of the *P. aeruginosa* type III effectors have been reported (20), it remains unclear how *P. aeruginosa* penetrates the epithelial cell barrier on the basis of interactions between type III effectors and such substrate proteins. Hauser previously suggested that the disruption of the cytoskeletal structure mediated by ExoS may contribute to a reduction in cell-cell adherence, which in turn may facilitate *P. aeruginosa* penetration through epithelial barriers, but there is no direct experimental confirmation of this hypothesis at present (20).

Our aim here was to reveal the precise molecular mechanism by which *P. aeruginosa* disrupts TJs and penetrates the epithelial cell barrier.

MATERIALS AND METHODS

Bacterial strains. *P. aeruginosa* PAO1 is our laboratory stock strain. The Δ*exoS* strain was constructed with suicide vector pEX18Tc as described previously (25). A 975-bp upstream sequence of the *exoS* gene was amplified with primers PA3841FF (5′-GGAATTCGCCCTGGCTCAGCCTGGT-3′) and PA3841FR (5′-TCGTGACGTCGATGGTTGCCTTCTCCTGATGTTTC-3′). A 945-bp downstream sequence of the *exoS* gene was amplified with primers PA3841BF (5′-GGCAACCATCGACGTCACGAACGGACACCTTG-3′) and PA3841BR (5′-TATCTAGAATCGCCGGCAGCCCGGAA-3′). These two flanking sequences were joined by fusion PCR as described previously (30). The fused gene was cloned into pEX18Tc (Δ*exoS*-pEX18Tc). Δ*exoS*-pEX18Tc was mobilized into PAO1 by conjugation. The Δ*exoS* strain was selected from transconjugants as described previously (25).

To construct the Δ*exoS*/*exoS* strain, a 69-bp DNA fragment containing the *tac* promoter region in plasmid pME6032 (21) was prepared by annealing two primers (5′-AATTCTGTTTCCTGTGTGAAATTGTTATCCGCTCACAATTCCACACATTATACGAGCCGATGATTAATTGTCAAC-3′ and 5′-TCGAGTTGACAATTAATCATCGGCTCGTATAATGTGTGGAATTGTGAGCGGATAACAATTTCACACAGGAAACAG-3′). The fragment was cloned into vector pBBR1MCS5 (29) (pBBR1MCS5-*tac*). A 1.6-kb fragment containing the *exoS* gene with its native promoter (PA3841; region at positions 4302981 to 4304502 of the PAO1 chromosome) was amplified by PCR with primers 5′-GTGGGAATTCGGCGTGTTCCGAGTCACTGG-3′ and 5′-AGAGGGATCCTCAGGCCAGATCAAGGCCGCGCATCCTCAG-3′. The PCR product was cloned into pBBR1MCS5-*tac*. The resulting plasmid was transformed into the Δ*exoS* strain.

P. aeruginosa strains PA23, PA46, PA71, PA73, and PA85 are clinical isolates derived from patient blood samples. The institutional review board at Kyoto Pharmaceutical University reviewed and approved this research using these human isolates.

Escherichia coli K-12 strain W3110 is a standard strain used for the genome analysis project in Japan (http://ecoli.aist-nara.ac.jp/GB5/search.jsp) and was used as a control strain that does not penetrate epithelial cell monolayers.

Comparative genomic hybridization (CGH) analysis. Total DNA (3 to 7 μg) isolated from cultures of *P. aeruginosa* strains PA23, PA46, PA71, PA73, and PA85 grown overnight was fragmented in 50 μl by adding 5 μl of 10× One-Phor-All buffer and DNase I (0.6 U/μg DNA). Fragmented DNA (ranging from 50 to 200 bp) was labeled with biotin-ddUTP. The resulting DNAs were hybridized to a *P. aeruginosa* PAO1 GeneChip (Affymetrix). DNA microarray analysis using a *P. aeruginosa* GeneChip was performed according to the manufacturer's instructions. The detected genes were identified in the *P. aeruginosa* PAO1 chromosome (www.pseudomonas.com).

Bacterial infection model using silkworms. The injection of bacteria (10^6 CFU per silkworm) into the hemolymph and midgut of 10 silkworms (Hu-Yo × Tukuba-Ne) at the fifth-instar stage was performed as described previously (19, 26, 28).

We developed an oral infection model using silkworms. Twenty silkworms at the fifth-instar stage were fed an antibiotic-free artificial food, Silkmate (an approximately 1.0-cm^3 block; Katakura Industries), to which 200 μl of a culture of *P. aeruginosa* (10^{10} CFU/ml) grown overnight had been added. As a negative control, 200 μl of saline was used. The silkworms were maintained without food, and survival was monitored for 5 days. The number of bacteria in the hemolymph at 1 h and 24 h after oral infection of three silkworms with strain PAO1 and the Δ*exoS* strain was measured by spreading 100 μl of hemolymph fluid onto LB agar. The results are expressed as means ± standard deviations (SD).

Viabilities after the direct injection of strain PAO1 and the Δ*exoS* strain into the hemolymphs of four silkworms were also compared.

Penetration assay. We carried out a penetration assay using MDCK monolayers at a multiplicity of infection (MOI) of 100 as described previously (24). The assay was performed in triplicate, and the results are expressed as means ± SD.

The bacterial association, invasion, and penetration assay at 3 h after infection was carried out as described previously (24). The assay was performed in triplicate, and the results are expressed as means ± SD.

Caco-2 cell monolayers in Transwell (Corning) plates were prepared at a density of 5.0×10^4 cells per cm^2 as described previously (39). Bacteria were inoculated at 5.0×10^6 CFU per well. The assay was performed in triplicate, and the results are expressed as means ± SD.

Apoptosis and cytotoxicity assay. Caco-2 cell monolayers in Transwell plates were infected at an MOI of 100 for 3 h and analyzed with the Cell Death Detection ELISA^{PLUS} kit (Roche) according to the manufacturer's instructions. The enrichment of mono- and oligonucleosomes released into the cytoplasm was calculated as the ratio of the absorbance of the sample cells to that of the control cells. The enrichment factor was used as a parameter of apoptosis and is shown on the *y* axis as the means ± SD from triplicate experiments. An enrichment factor of 1 represents background or spontaneous apoptosis.

Caco-2 cells in 96-well plates were infected at an MOI of 100 for 3 h and analyzed with the Cytotoxicity Detection Kit^{PLUS} (LDH) (Roche) according to the manufacturer's instructions. The assay was performed in triplicate, and the results are expressed as the means ± SD.

Bacterial two-hybrid assay. A BacterioMatch II two-hybrid assay employing a human colon cDNA library (Stratagene) was carried out according to the manufacturer's instructions. pBT-*exoS* was constructed by inserting the full-length *exoS* gene amplified by PCR with primers (5′-GAAGGCGGCCGCAATGCATATTCAATCGCTTCAG-3′ and 5′-AGAGGAATTCTCAGGCCAGATCAAGGCCGCGCATCCTCAG-3′) into the pBT vector. Transformants were selected with a His3 reporter by selective plates containing 3-amino-1,2,4-triazole (3AT).

Pulldown assay. pGST-ExoS was constructed by cloning the full-length *exoS* gene, amplified by PCR with primers (5′-GGCCGGATCCATGCAGAAGGTGACCCTGGG and 5′-GCGCGAATTCTCAGCTTTGGGCTGAGCCTG), into pGEX-6P-1 (Amersham Pharmacia Biotech). The glutathione *S*-transferase

(GST) fusion (ExoS) protein was purified as described previously (40) and used for the pulldown assay after removal of the GST tag.

pGST-FXYD3 was constructed by cloning the full-length FXYD3 gene, amplified by PCR with primers 5′-GGCCGGATCCATGCAGAAGGTGACCCTGGG and 5′-AGAGGAATTCTCAGCTTTGGGCTGAGCCTGGGGTGATGAG, into pGEX-6P-1. Each deleted FXYD3 gene was amplified by PCR with primers 5′-CATCGGATCCGCAAAATGCAAATGCAAGTTTGGC and 5′-GCGCGAATTCTCAGCTTTGGGCTGAGCCTG for GST-FXYD3 (exons 7, 8, and 9), 5′-GGCCGGATCCATGCAGAAGGTGACCCTGGG and 5′-AGGCGAATTCTCAATAGTAGAAAGGATCGTTTTTATCTTCTAG for GST-FXYD3 (signal peptide plus exons 4 and 5), 5′-GGCCGGATCCATGCAGAAGGTGACCCTGGG and 5′-CAAAGAATTCTCAGCATTTTGCACTCATGACGATGATG for GST-FXYD3 (signal peptide plus exons 4, 5, and 6), and 5′-CCTGGGATCCAATGACCTAGAAGATAAAAACAGTCC and 5′-GCGCGAATTCTCAGCTTTGGGCTGAGCCTG for GST-FXYD3 (exons 4, 5, 6, 7, 8, and 9) and cloned into pGEX-6P-1. GST-FXYD3 and GST-deleted FXYD3 proteins were expressed in *E. coli* cells as inclusion bodies and purified as described previously (40). Purified GST-FXYD3 proteins were used for the pulldown assay.

In Fig. 3A, GST-FXYD3 or GST alone immobilized on glutathione-Sepharose beads was incubated with the full-length ExoS protein. The pulled-down proteins were analyzed by Western blotting using an anti-ExoS antibody.

In Fig. 3B, GST-FXYD3, GST-FXYD3 (exons 7, 8, and 9), GST-FXYD3 (signal peptide plus exons 4 and 5), GST-FXYD3 (signal peptide plus exons 4, 5, and 6), GST-FXYD3 (exons 4, 5, 6, 7, 8, and 9), or the GST protein alone was immobilized on glutathione-Sepharose beads and incubated with full-length ExoS. The pulled-down proteins were subjected to Western blot analysis using an anti-ExoS antibody.

Antibodies. Anti-ExoS polyclonal antibody was prepared by immunizing a rabbit with a mixture of two synthetic oligopeptides corresponding to amino acids 75 to 91 (LLGSHARTGPQPSQDAQ) and 428 to 443 (LASKPERSGEVQEQDV) of the ExoS protein. Anti-FXYD3 rabbit and goat antibodies were obtained from Santa Cruz Biotechnology. Anti-ZO-1, anti-occludin, anti-E-cadherin, and anti-β-catenin antibodies were obtained from Invitrogen. Anti-β-actin antibody was obtained from Chemicon.

Targeting of FXYD3 with artificial microRNAs. We designed two FXYD3 targeting sequences, 229-miRNA (5′-TGCTGTCTTCTAGGTCATTGGCGTCCGTTTTGGCCACTGACTGACGGACGCCAGACCTAGAAGA and 5′-CCTGTCTTCTAGGTCTGGCGTCCGTCAGTCAGTGGCCAAAACGGACGCCAATGACCTAGAAGAC) and 232-miRNA (5′-TGCTGTTATCTTCTAGGTCATTGGCGGTTTTGGCCACTGACTGACCGCCAATGCTAGAAGATAA and 5′-CCTGTTATCTTCTAGCATTGGCGGTCAGTCAGTGGCCAAAACCGCCAATGACCTAGAAGATAAC), on the basis of data under GenBank accession no. NM_005971.2. These double-stranded microRNA (miRNA) genes were ligated with the Block-iT Pol II miR RNA interference (RNAi) expression vector (Invitrogen). Plasmids expressing either of the two FXYD3 miRNAs or the control miRNA (pcDNA6.2-GW/EmGFP-miR-neg control vector; Invitrogen) were transfected into Caco-2 cells by using the FuGene HD kit (Roche), and stable transfectants were selected based on green fluorescent protein (GFP) fluorescence and blasticidin resistance.

Penetration assay using FXYD3-KD-Caco-2 cell monolayers. Caco-2 cells in which FXYD3 expression had been knocked down following transfection and the stable expression of either of the two FXYD3-miRNAs (FXYD3-KD-Caco-2) or Caco-2 cells expressing the control miRNA (control-Caco-2) were seeded onto a 12-well Transwell at a density of 5.0×10^4 cells per cm^2 and incubated for ~2 weeks until the transepithelial resistance (TER) reached 500 $\Omega \cdot cm^2$. Both FXYD3-KD-Caco-2 and control-Caco-2 cells were infected at an MOI of 100, and the number of bacteria in the basolateral medium was counted. The assay was performed in triplicate, and the results are expressed as means ± SD.

Na,K-ATPase activity. Membrane preparations from FXYD3-KD-Caco-2 and control-Caco-2 cells were prepared as follows: cells were collected and centrifuged at 3,000 × *g* for 10 min (about 1 ml of packed cells). The cell pellet was resuspended in 10 ml of 250 mM sucrose buffer containing 10 mM Tris-HCl (pH 7.5) and Complete protease inhibitor cocktail (Roche). The cells were thawed rapidly, the cell lysate was centrifuged at 800 × *g* for 5 min, and the pellet was resuspended in 5 ml of 1 mM Na_2CO_3 at room temperature. The volume was brought to 40 ml with 1 mM Na_2CO_3, and the homogenate was incubated for 5 min at room temperature. The homogenate was centrifuged for 10 min at 800 × *g*, and the supernatant was ultracentrifuged at 100,000 × *g* for 30 min at 4°C. After resuspending the resultant pellet in 0.5 ml of 10 mM Tris-HCl (pH 7.5), sucrose solutions (9 ml of 45% sucrose, 9 ml of 31% sucrose, and 6 ml of 9% sucrose) were added carefully to form separate layers, and sucrose density gradient centrifugation was then carried out at 100,000 × *g* for 3 h at 4°C. The bands at the boundaries between 9% and 31% and between 31% and 45% were collected and ultracentrifuged at 100,000 × *g* for 30 min at 4°C. The pellet was resuspended in 10% glycerol, and the resulting membrane suspension was used as the membrane protein in the Na,K-ATPase assay described below.

The Na,K-ATPase activity was measured as described previously (43). The Na,K-ATPase activity of the membrane protein was assayed in reaction mixtures of (i) 30 mM imidazole-HCl, 130 mM NaCl, 20 mM KCl, and 4 mM $MgCl_2$ and (ii) 30 mM imidazole-HCl, 4 mM $MgCl_2$, and 1 mM ouabain, at pH 7.4, each containing 20 μg of membrane protein. For complete ouabain binding, the tubes were preincubated for 1 h at room temperature. The reaction was started by adding 4 mM Tris-ATP (Sigma) to the mixture, and the mixture was incubated for 30 min at 37°C. The amount of P_i formed was determined by using Biomol green reagent (Biomol Research Laboratories) according to the manufacturer's instructions. The Na,K-ATPase activity was calculated as the difference in the P_i content (μM/mg protein/h) between reaction mixtures i and ii. Determination of Na,K-ATPase activity in the presence of ExoS was carried out by the addition of purified ExoS (25 μg) to reaction mixtures i and ii.

Expression of ZO-1 and occludin in Caco-2 cell monolayers infected with PAO1 and the Δ*exoS* and Δ*exoS*/*exoS* strains. Caco-2 cell monolayers were used when their TER values were >500 $\Omega \cdot cm^2$. Caco-2 monolayers were infected at an MOI of 100 and incubated for 4 h at 37°C. The cell lysates prepared with radioimmunoprecipitation assay (RIPA) buffer (Pierce) were analyzed by Western blotting using anti-ZO-1, anti-occludin, and anti-β-actin antibodies.

Confocal microscopy. FXYD3-KD-Caco-2 and control-Caco-2 cells or Caco-2 cells infected with bacteria were stained with anti-ZO-1 and anti-occludin antibodies. Cells were fixed in 4% paraformaldehyde, treated with NH_4Cl, and permeabilized with 0.2% Triton X-100. Cells were incubated with anti-ZO-1 rabbit and anti-occludin rabbit antibodies. After washing with Tris-buffered saline–Tween (TBS-T), cells were incubated with Alexa Fluor 546 anti-rabbit IgG (Invitrogen). Cells were examined by using a confocal laser scanning microscope (LSM510 Meta; Carl Zeiss).

Caco-2 cells infected with PAO1, the Δ*exoS* strain, and *Escherichia coli* strain W3110 were double stained with anti-ExoS rabbit antibody plus Alexa Fluor 594 anti-rabbit IgG and anti-FXYD3 goat antibody plus Alexa Fluor 488 anti-goat IgG as described above.

***In vivo* immunoprecipitation of endogenous FXYD3.** Caco-2 cells infected with PAO1 and the Δ*exoS* strain or uninfected Caco-2 cells were treated with 2.5 mM DSP [dithiobis(succinimidylpropionate)]. The cells were lysed by using a M-PER kit (Pierce), and the cell lysates were diluted with M-PER buffer (Pierce) and treated with either anti-FXYD3 rabbit antibody or normal rabbit serum. The immune complexes were trapped by using PureProteome protein A magnetic beads (Millipore) and analyzed by Western blotting using anti-ExoS and anti-FXYD3 rabbit antibodies.

Statistical analysis. Statistical analysis was performed by using a two-tailed *t* test. In Fig. 1B, the log-rank test was applied for testing the differences between the survival curves. JMP statistical analysis software, version 7.0 (SAS Institute, NC), was used.

RESULTS

Comparison of the virulences of clinical blood isolates of *P. aeruginosa* toward silkworms. A positive correlation between the virulences of *P. aeruginosa* in mammals and insects has been reported (6, 19, 26, 27, 32, 33). Therefore, we compared the virulences of five clinical blood isolates by injecting the bacteria into the midgut and hemolymph of silkworms. The virulence of strain PA46 was greater than those of the other four strains following injection into either location. Strain PA46 killed all silkworms by 54 h following midgut injection and by 30 h following hemolymph injection, whereas the other strains required more than 72 h and 63 h, respectively, to do the same (data not shown). The greater virulence of strain PA46 particularly following midgut injection suggests that it is able to more efficiently penetrate the intestinal barrier comprising the epithelial cell layer. Penetration through the intestinal barrier is considered a key factor associated with the ability of the bacterium to initiate gut-derived sepsis (24).

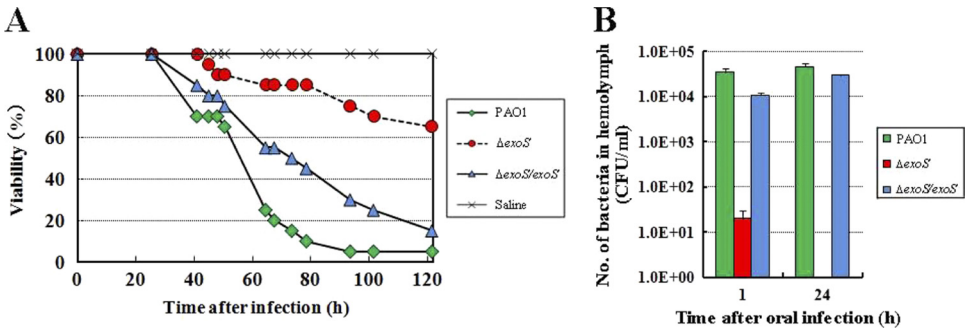

FIG. 1. The type III effector ExoS is essential for *P. aeruginosa* virulence against silkworms, due to its ability to mediate penetration through the midgut barrier. (A) Comparison of the virulences of PAO1 and the Δ*exoS* and Δ*exoS*/*exoS* strains or saline following oral administration to 20 silkworms. The log-rank test suggested significant differences between the virulence of the wild-type strain and that of the Δ*exoS* strain (chi-squared value of 22.069; $P < 0.0001$) and between the virulence of the Δ*exoS* strain and that of the Δ*exoS*/*exoS* strain (chi-squared value of 11.097; $P = 0.0009$). Although the multiplicity problem in the log-rank test was considered, we concluded that the differences in these combinations could be considered significant because of the sufficiently low *P* values. (B) Numbers of bacteria in the hemolymph at 1 h and 24 h after oral administration of PAO1 and the Δ*exoS* and Δ*exoS*/*exoS* strains to three silkworms. There was a significant difference between numbers of PAO1 and Δ*exoS* strain bacteria detected at 1 h and 24 h after oral infection ($P < 0.05$ and $P < 0.001$, respectively). There was also a significant difference between the numbers of Δ*exoS*/*exoS* and Δ*exoS* strain bacteria detected at 1 h and 24 h after oral infection ($P < 0.02$ and $P < 0.001$, respectively).

CGH analysis of clinical blood isolates. To identify genes associated with bacterial translocation from the midgut to the hemolymph of silkworms, we performed comparative genomic hybridization (CGH) analysis on strain PA46, which showed higher virulence in silkworms following midgut injection, and on the other strains, which exhibited lower virulence (data not shown). This analysis identified 61 genes that were specifically detected in strain PA46 (data not shown). Among these 61 genes, we focused our attention on the *exoS* gene (PA3841), since the contribution of the type III effector ExoS to the ability of *P. aeruginosa* to penetrate the intestinal epithelial cell barrier is not well known. We constructed an *exoS* knockout strain (designated the Δ*exoS* strain) from *P. aeruginosa* PAO1 (the wild-type strain) and analyzed its virulence using a silkworm oral infection model. We generated the Δ*exoS* strain from wild-type strain PAO1 instead of strain PA46 owing to the difficulty in the genetic manipulation of the latter.

The virulence of the Δ*exoS* strain was significantly attenuated compared to the wild type and Δ*exoS*-complemented strain (the Δ*exoS*/*exoS* strain) (Fig. 1A). This result suggests that ExoS is required for *P. aeruginosa* virulence in silkworms. We next evaluated directly the ability of the wild-type, Δ*exoS*, and Δ*exoS*/*exoS* strains to penetrate the midgut barrier after oral administration. As shown in Fig. 1B, the numbers of wild-type and Δ*exoS*/*exoS* bacteria identified in the hemolymph at 1 h and 24 h after oral infection were significantly greater than that of Δ*exoS* bacteria. We also compared the abilities of the wild-type and Δ*exoS* strains to grow or survive following direct injection into the hemolymph. Viabilities following injection into the hemolymph were similar between the two strains at all inoculum doses tested (10^7 to 10^1 CFU/silkworm) (data not shown). Therefore, we conclude that the high mortality of silkworms following oral administration of the wild-type strain is dependent upon the ability of the bacteria to penetrate efficiently through the midgut barrier in a manner dependent upon ExoS and that this effect is independent of the viability of the bacteria in the hemolymph.

Penetration assay. We next performed a penetration assay using an *in vitro*-cultured cell monolayer system (24) to determine whether the *exoS* gene is also necessary for the penetration of *P. aeruginosa* through an epithelial cell monolayer. Bacteria were inoculated onto the apical surfaces of MDCK cell monolayers at an MOI of 100, and the number of bacteria in the basolateral medium was counted at the indicated times. The Δ*exoS* strain exhibited a reduced ability to penetrate the MDCK cell monolayer relative to the penetration by the wild-type strain at all times following infection ($P < 0.05$) (Fig. 2A). We observed a good correlation between changes in the transepithelial resistance (TER) (Fig. 2B) and the number of bacteria that had penetrated through the MDCK monolayers over time (Fig. 2A). TER is a sensitive measure of tight junctional barrier function and reflects the condition of tight junction formation. There was a steep drop in the TER of MDCK monolayers infected with the wild-type strain.

We next aimed to distinguish between two possible routes by which PAO1 penetrates the MDCK cell monolayer: passage through the paracellular spaces between the cells and invasion of the cells from the apical side followed by release through the basolateral side. We observed that 0.03% of the wild-type bacterial inoculum had invaded the cells, whereas 0.23% of the bacteria had penetrated through the monolayers (Fig. 2C, D, E, and F). These results suggest that a greater fraction of PAO1 bacteria penetrated the MDCK cell monolayers through the paracellular spaces than by the direct invasion of the cells.

We next performed a penetration assay using Caco-2 colon epithelial cells, which are of human origin. Bacteria of the Δ*exoS* strain penetrated Caco-2 cell monolayers much less efficiently than did those of the wild-type strain at either 3 or 4 h following infection ($P < 0.05$) (Fig. 2G). The decrease in the ability of the Δ*exoS* strain to penetrate the monolayers was largely restored in the Δ*exoS*/*exoS* strain ($P < 0.05$) (Fig. 2G). There was no significant difference in apoptosis or cytotoxicity in Caco-2 cells at 3 h after infection with bacteria of either the wild-type or Δ*exoS* strain (Fig. 2H and I).

ExoS binds to FXYD3. TJs seal the paracellular spaces between epithelial cells and function as an epithelial barrier to prevent bacterial penetration from the intestine into the bloodstream. If PAO1 penetrates epithelial cell monolayers predom-

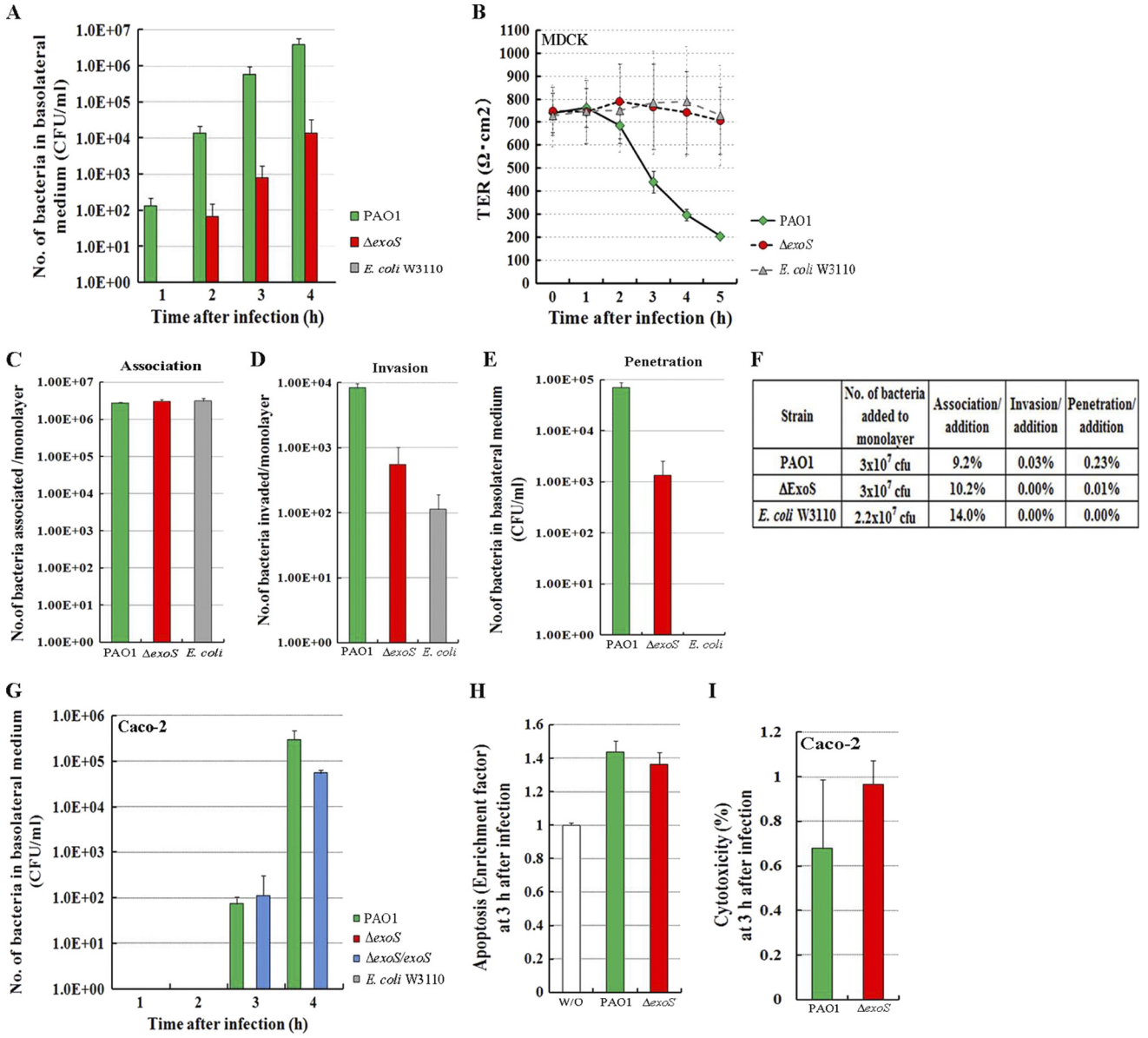

Strain	No. of bacteria added to monolayer	Association/ addition	Invasion/ addition	Penetration/ addition
PAO1	$3x10^7$ cfu	9.2%	0.03%	0.23%
ΔExoS	$3x10^7$ cfu	10.2%	0.00%	0.01%
E. coli W3110	$2.2x10^7$ cfu	14.0%	0.00%	0.00%

FIG. 2. ExoS is necessary for penetration of *P. aeruginosa* through epithelial cell monolayers *in vitro*. (A) Penetration of PAO1, the Δ*exoS* strain, and *E. coli* W3110 through MDCK cell monolayers. Bacteria (10^8 CFU) were inoculated onto the apical surfaces of MDCK cell monolayers (10^6 cells) at an MOI of 100, and the number of bacteria in the basolateral medium was counted at the indicated times. The assay was performed in triplicate, and the results are expressed as means ± SD. (B) Change in the TER following infection of MDCK cell monolayers with PAO1, the Δ*exoS* strain, and *E. coli* W3110 at an MOI of 100. The TER was measured at the indicated times in triplicate and is expressed as the average ± SD of the resistance multiplied by the area. (C) Bacterial association with MDCK cell monolayers. Bacterial association was evaluated by the lysis of MDCK cells infected with PAO1, the Δ*exoS* strain, and *E. coli* W3110 at an MOI of 100 with Triton X-100 at 3 h after infection. The assay was carried out in triplicate, and results are expressed as means ± SD. There was no significant difference between PAO-infected and Δ*exoS* strain-infected MDCK cell monolayers ($P > 0.1$). (D) Bacterial invasion into MDCK cell monolayers. Bacterial invasion was evaluated by the lysis of MDCK cells infected with PAO1, the Δ*exoS* strain, and *E. coli* W3110 at an MOI of 100 with Triton X-100 at 3 h after infection but after treatment with 200 μg/ml of gentamicin for 2 h to kill extracellular bacteria. The assay was carried out in triplicate, and results are expressed as means ± SD. There was a significant difference between PAO-infected and Δ*exoS* strain-infected MDCK cell monolayers ($P < 0.001$). (E) Bacterial penetration through MDCK cell monolayers. Bacteria (10^8 CFU) were inoculated onto the apical surfaces of MDCK cell monolayers (10^6 cells) at an MOI of 100, and the number of bacteria in the basolateral medium was counted at 3 h after infection. The assay was carried out in triplicate, and the results are expressed as means ± SD. There was a significant difference between PAO-infected and Δ*exoS* strain-infected MDCK cell monolayers ($P < 0.005$). (F) Association, invasion, and penetration rates expressed as percentages of the numbers of bacteria added to the monolayers on the basis of the results shown in C, D, and E. (G) Penetration of PAO1, the Δ*exoS* strain, the Δ*exoS*/*exoS* strain, and *E. coli* W3110 through Caco-2 human colon epithelial cell monolayers. Bacteria were inoculated onto the apical surfaces of Caco-2 cell monolayers at an MOI of 100, and the number of bacteria in the basolateral medium was counted at the indicated times. The assay was performed in triplicate, and the results are expressed as means ± SD. (H) Apoptosis of Caco-2 cell monolayers infected with PAO1 and the Δ*exoS* strain at an MOI of 100 for 3 h. There was no significant difference between PAO-infected and Δ*exoS* strain-infected Caco-2 cell monolayers ($P > 0.1$). W/O, without infection. (I) Cytotoxicity assay of Caco-2 cells in 96-well plates infected with PAO1 and the Δ*exoS* strain at an MOI of 100 for 3 h. There was no significant difference between PAO-infected and Δ*exoS* strain-infected Caco-2 cell monolayers ($P > 0.1$).

TABLE 1. Homologs of the cDNAs isolated from positive clones upon bacterial two-hybrid screening

Homolog in database	No. of clones isolated	GenBank accession no.	Expectation value
Mitochondrion, complete genome	4	NC_001807.4	0.0
Myosin, heavy chain 11, smooth muscle (MYH11), transcript variant SM2A, mRNA	3	NM_022844.2	0.0
FXYD domain-containing ion transport regulator 3 (FXYD3), transcript variant 1, mRNA	2	NM_005971.2	0.0
Proliferation-associated 2G4, 38 kDa (PA2G4), mRNA	1	NM_006191.2	0.0
Hypothetical LOC730415, transcript variant 2 (LOC730415), mRNA	1	XM_001720835.1	0.0
Zinc finger, DHHC-type containing 3 (ZDHHC3), mRNA	1	NM_016598.1	0.0
Vacuolar protein-sorting 28 homolog (*S. cerevisiae*) (VPS28), transcript variant 1, mRNA	1	NM_016208.2	0.0
Globoside alpha-1,3-*N*-acetylgalactosaminyltransferase 1 (GBGT1), mRNA	1	NM_021996.4	0.0
Chromosome 12 genomic contig	1	NT_009714.16	0.0
Family with sequence similarity 44, member A, mRNA (cDNA clone IMAGE accession no. 4395670)	1	BC016987.1	0.0
Signal transducer and activator of transcription 6, interleukin-4 induced (STAT6), mRNA	1	NM_003153.3	0.0
Transmembrane protein 103 (TMEM103), mRNA	1	NM_001031703.2	0.0
Actin, gamma 1 (ACTG1), mRNA	1	NM_001614.2	0.0
Major histocompatibility complex class I, E (HLA-E), mRNA	1	NM_005516.4	0.0
Ring finger protein 123 (RNF123), mRNA	1	NM_022064.2	0.0
Myosin IC (MYO1C), transcript variant 2, mRNA	1	NM_001080950.1	0.0
Dynactin 2 (p50) (DCTN2), mRNA	1	NM_006400.3	1E−179
Haplotype H5 mitochondrion, complete genome	1	EU677750.1	4E−166
Xylulokinase homolog (*Haemophilus influenzae*) (XYLB), mRNA	1	NM_005108.2	2E−119
Creatine kinase, brain (CKB), mRNA	1	XM_510185.2	2E−101

inantly through the paracellular spaces, they likely impair the function of TJs by some unknown mechanism. Since the ability of the Δ*exoS* strain to penetrate epithelial cell monolayers is strongly attenuated, we hypothesized that PAO1 injects ExoS into epithelial cells and that the injected ExoS binds a host factor associated with TJ formation to disrupt the TJ structure. To identify the host protein(s) that binds ExoS, we performed a yeast two-hybrid screen. This effort was unsuccessful due to the lethal effect of ExoS expression on *Saccharomyces cerevisiae* cells (45). In contrast, a bacterial two-hybrid screen ($>5 \times 10^5$ clones from a human colon cDNA library) identified 26 positive clones. The cDNA sequences of the 26 positive clones are listed in the Table 1. Among 26 positive clones, we focused on FXYD domain-containing ion transport regulator 3 (FXYD3) (GenBank accession no. NM_005971.2), since FXYD3 is known to be associated with TJ formation (3, 10, 42). The interaction of ExoS with FXYD3 was confirmed by using a GST pulldown assay (40). GST-FXYD3 bound to ExoS (Fig. 3A).

The transmembrane domain of FXYD3 interacts with ExoS. FXYD3 is a member of the FXYD family of membrane proteins, which possess a single transmembrane domain (50). Its secondary structure was determined by nuclear magnetic resonance (NMR) performed on the protein prepared in lipid micelles, and it was found that its structure comprises four helical domains (13, 14) (H1 to H4) (Fig. 3C). In addition, an Na,K-ATPase interaction domain was predicted from the three-dimensional NMR structure of FXYD1 (13) (Fig. 3C). We determined which domain of FXYD3 binds to ExoS by using a GST pulldown assay. As shown in Fig. 3B and C, neither GST-FXYD3 (signal peptide plus exons 4 and5) nor GST-FXYD3 (exons 7, 8, and 9) bound ExoS, whereas GST-FXYD3 (signal peptide plus exons 4, 5, and 6) and GST-FXYD3 (exons 4, 5, 6, 7, 8, and 9) did, which suggests that the transmembrane domain of FXYD3 binds to ExoS (H1 and H2 helix region [exon 6] (Fig. 3C). However, we cannot rule out the possibility that the deletion of the transmembrane domain of FXYD3 may disrupt the overall folding of this protein and thereby interfere with the binding of this protein to ExoS.

Proteins of the FXYD family function as tissue-specific modulators of Na,K-ATPase activity. The inhibition of Na,K-ATPase activity at TJs is known to induce a rearrangement of TJ strands and to increase the permeability of TJs to ionic and nonionic solutes in pancreatic epithelial cells, which suggests that Na,K-ATPase is essential for controlling TJ gate function (42). These facts led us to hypothesize that the binding of ExoS to FXYD3 may lead to the inactivation of FXYD3, thereby inhibiting Na,K-ATPase activity to impair TJ gate function against *P. aeruginosa* penetration. To confirm this hypothesis, we investigated whether the silencing of FXYD3 expression in Caco-2 cells could influence the TJ structure and its barrier function.

Silencing of FXYD3 expression in Caco-2 cells disrupts both the tight junction structure and its barrier function against bacterial penetration. The TJs and adherens junctions (AJs) comprise a complex of proteins that function as a barrier to the diffusion of macromolecules across epithelial cells. TJs and AJs are localized on the apical and basolateral sides of the epithelial cells, respectively, where they mediate the barrier function independent of one another. Whereas TJs constitute the main physical barrier to the diffusion of molecules through the paracellular space, AJs may indirectly regulate the structure and function of TJs (47). The occludin and ZO-1 proteins are structural components of the TJs that seal the paracellular spaces between the cells and function as the epithelial barrier (7), whereas the main molecular component of AJs is E-cadherin, which is connected to the actin cytoskeleton via cytoplasmic α-, β-, and γ-catenins. We performed miRNA-mediated FXYD3 gene silencing in Caco-2 cells, since the expression of the FXYD3 gene in Caco-2 cells has been confirmed (4). In Caco-2 cells, the constitutive expression of either of two miRNAs (229-miRNA and 232-miRNA) designed to

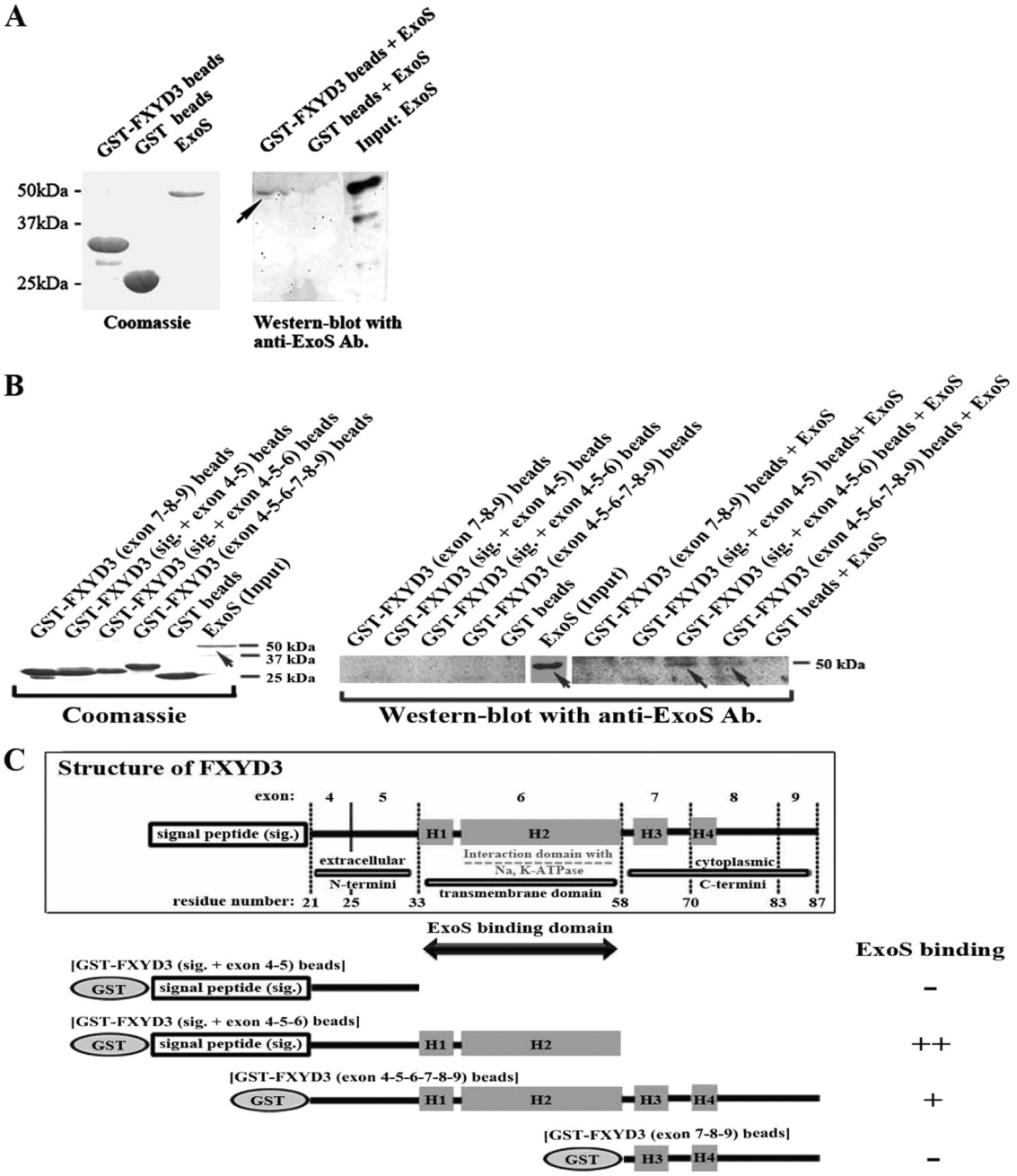

FIG. 3. ExoS binds to FXYD3, a regulator of Na,K-ATPase. (A) Interaction of ExoS with FXYD3 *in vitro*. GST-FXYD3 or GST alone immobilized on glutathione-Sepharose beads was incubated with full-length ExoS. The pulled-down proteins were analyzed by Western blotting using an anti-ExoS antibody (Ab.). The arrow indicates the presence of the ExoS protein on the Western blot. Coomassie brilliant blue staining of the proteins analyzed by SDS-PAGE is shown at the left. (B) Determination of the region of FXYD3 that mediates binding to ExoS. Coomassie brilliant blue staining of the various GST-FXDY3 deletion mutants analyzed by SDS-PAGE is shown at the left. sig., signal peptide. GST-FXYD3, GST-FXYD3 (exons 7, 8, and 9), GST-FXYD3 (signal peptide plus exons 4 and 5), GST-FXYD3 (signal peptide plus exons 4, 5, and 6), GST-FXYD3 (exons 4, 5, 6, 7, 8, 9), or the GST protein alone was immobilized on glutathione-Sepharose beads and incubated with full-length ExoS. The pulled-down proteins were subjected to Western blot analysis using an anti-ExoS antibody. The arrows indicate the bound ExoS protein analyzed by Western blotting. (C) Schematic representation of the structure of FXYD3 (38) and the ExoS-binding domain. ExoS binding is a summary of the results shown in B and is indicated schematically by minuses and pluses.

specifically target different regions of the FXYD3 gene led to greatly reduced levels of expression of the FXYD3 gene (98% suppression) compared to that observed for cells expressing a control miRNA vector (Fig. 4A). In Caco-2 cells in which FXYD3 expression was knocked down, we observed greatly reduced expression levels of occludin and ZO-1 (94% and 98% reductions, respectively) (Fig. 4A). In contrast, there was no significant difference in the expression levels of β-catenin or

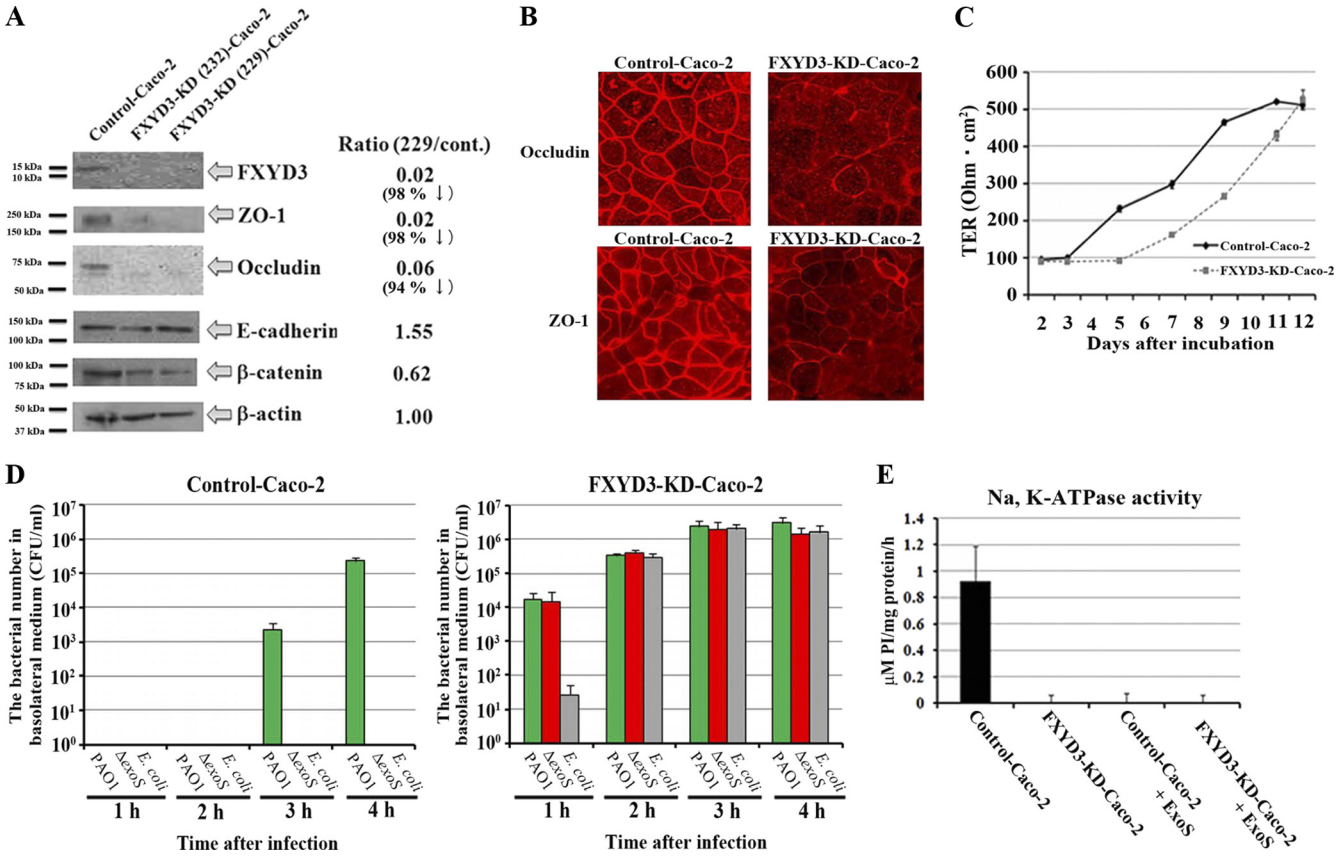

FIG. 4. Knockdown of FXYD3 expression influences the structure and barrier functions of tight junctions against bacterial penetration in Caco-2 cells. (A) Western blot analysis of cell lysates prepared from Caco-2 cells constitutively expressing either 229-miRNA or 232-miRNA, which are specific for the FXYD3 gene, or constitutively expressing a control plasmid. Proteins were detected with anti-FXYD3, anti-ZO-1, anti-occludin, anti-E-cadherin, anti-β-catenin, or anti-β-actin antibodies. Normalized expression ratios were compared between control and FXYD3-KD (229)-Caco-2 cells. Protein expression was standardized to the level of expression of the β-actin protein. (B) Confocal images of control and FXYD3 knockdown Caco-2 cells analyzed by immunofluorescence for the expression of occludin and ZO-1. FXYD3-KD-Caco-2 and control-Caco-2 cells were fixed in 4% paraformaldehyde, treated with NH_4Cl, and permeabilized with 0.2% Triton X-100. Cells were incubated with anti-ZO-1 rabbit and anti-occludin rabbit antibodies. After washing with TBS-T, cells were incubated with Alexa Fluor 546 anti-rabbit IgG. Cells were examined by using a confocal laser scanning microscope. (C) Changes in the TERs of control and FXYD3 knockdown Caco-2 cells. The TER was measured on the indicated days in triplicate and is expressed as the average ± SD of the resistance multiplied by the area. (D) Penetration of PAO1, the Δ*exoS* strain, and *E. coli* W3110 through control (left) and FXYD3 knockdown (right) Caco-2 cell monolayers. Both control-Caco-2 and FXYD3-KD-Caco-2 cells were infected at an MOI of 100, and the number of bacteria in the basolateral medium was counted. The assay was performed in triplicate, and the results are expressed as means ± SD. In control monolayers, there was a significant difference between the extents of penetration by PAO1 and the Δ*exoS* strain ($P < 0.05$ at 3 h and $P < 0.002$ at 4 h) and between the extents of penetration by PAO1 and *E. coli* W3110 ($P < 0.05$ at 3 h and $P < 0.002$ at 4 h). In FXYD3 knockdown monolayers, there were similar levels of penetration by bacteria of PAO1 and the Δ*exoS* strain at all time points ($P > 0.1$) and between bacteria of PAO1 and *E. coli* W3110 at 2 h, 3 h, and 4 h after infection ($P > 0.1$), although there was a significant difference between the extents of penetration by PAO1 and *E. coli* W3110 at only 1 h after infection ($P < 0.05$). (E) Na,K-ATPase activity in control and FXYD3 knockdown Caco-2 cells in the absence or presence of ExoS (25 μg). The assay was performed in triplicate, and the results are expressed as means ± SD. PI, inorganic phosphate.

E-cadherin between the FXYD3 knockdown and control cells (Fig. 4A). Furthermore, confocal microscopy revealed that the silencing of FXYD3 in Caco-2 cells results in a TJ disruption due to a reduced level of expression of the TJ-associated proteins occludin and ZO-1 (Fig. 4B).

We next evaluated the effect of the knockdown of FXYD3 expression in Caco-2 cells on bacterial penetration. If PAO1 penetrates Caco-2 cell monolayers mediated by an interaction of ExoS with FXYD3 that impairs FXYD3 function, then the silencing of FXYD3 expression should facilitate the penetration of the Δ*exoS* strain through Caco-2 monolayers. First, we investigated whether FXYD3 knockdown cells form a normal monolayer by measuring the TER. As described previously (39), an increase in the TER to more than 300 $\Omega \cdot cm^2$ indicates the formation of a normal monolayer in Transwell plates. We observed an increase in the TER in both FXYD3 knockdown and control Caco-2 cells, although the TER of the FXYD3 knockdown cells increased more slowly than that of the control cells (Fig. 4C). However, since the TERs of both cell lines reached approximately 500 $\Omega \cdot cm^2$ by 12 days after seeding, we considered that normal monolayers had formed in both lines and performed the penetration assay. As shown in Fig. 4D, whereas only strain PAO1 could penetrate the control Caco-2 cell monolayers at 3 h and 4 h after infection, in the FXYD3 knockdown cells, the Δ*exoS* strain recovered the ability to penetrate the monolayers at all time points to an extent

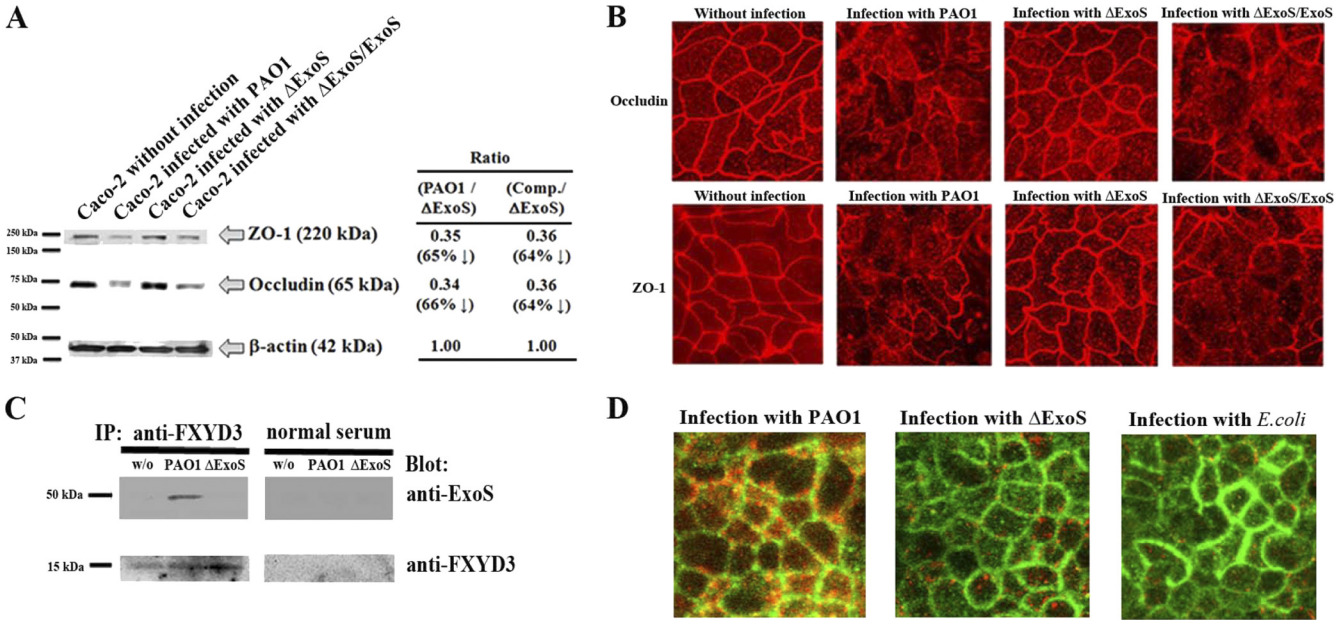

FIG. 5. Infection of Caco-2 cells with PAO1 disrupts tight junction structure through binding of ExoS to endogenous FXYD3. (A) Expression of ZO-1 and occludin in Caco-2 cell monolayers infected with PAO1 and the Δ*exoS* and Δ*exoS*/*exoS* strains. Caco-2 monolayers were infected at an MOI of 100 and incubated for 4 h at 37°C. The cell lysates were analyzed by Western blotting using anti-ZO-1, anti-occludin, and anti-β-actin antibodies. Normalized expression ratios were compared between PAO1-infected Caco-2 cells and Δ*exoS* strain-infected Caco-2 cells or between Δ*exoS*/*exoS* strain-infected Caco-2 cells and Δ*exoS* strain-infected Caco-2 cells. Protein expression was standardized to the expression of β-actin. (B) Confocal images of Caco-2 cell monolayers infected with PAO1 and the Δ*exoS* and Δ*exoS*/*exoS* strains and stained for occludin and ZO-1. Caco-2 cells infected with bacteria were fixed in 4% paraformaldehyde, treated with NH_4Cl, and permeabilized with 0.2% Triton X-100. Cells were incubated with anti-ZO-1 rabbit and anti-occludin rabbit antibodies. After washing with TBS-T, cells were incubated with Alexa Fluor 546 anti-rabbit IgG. Cells were examined by using a confocal laser scanning microscope. (C) *In vivo* immunoprecipitation (IP) of endogenous FXYD3 complexes. Caco-2 cells infected with PAO1 and the Δ*exoS* strain or uninfected Caco-2 cells were treated with 2.5 mM DSP. The cell lysates were treated with either anti-FXYD3 rabbit antibody or normal rabbit serum. The immune complexes were trapped by using protein A magnetic beads and analyzed by Western blotting using anti-ExoS and anti-FXYD3 rabbit antibodies. (D) Colocalization of ExoS and endogenous FXYD3 in Caco-2 cell monolayers infected with PAO1 but not in Caco-2 cell monolayers infected with the Δ*exoS* strain or *E. coli* W3110. Caco-2 cells infected with PAO1, the Δ*exoS* strain, and *E. coli* W3110 were double stained with anti-ExoS rabbit antibody plus Alexa Fluor 594 anti-rabbit IgG and anti-FXYD3 goat antibody plus Alexa Fluor 488 anti-goat IgG.

similar to that of PAO1 ($P > 0.1$) (Fig. 4D). In addition, *E. coli* W3110 cells were also able to penetrate monolayers of FXYD3 knockdown Caco-2 cells to an extent similar to that of PAO1 at 2 h, 3 h, and 4 h after infection ($P > 0.1$) (Fig. 4D). These results suggest that FXYD3 plays a key role in the regulation of TJ function as a barrier against bacterial penetration and that the impairment of FXYD3 function facilitates penetration through the monolayers due to a disruption of the TJs.

FXYD3 silencing and exposure of Caco-2 cells to ExoS both cause an inactivation of Na,K-ATPase activity. FXYD3 is known to regulate Na,K-ATPase activity (10). Recently, it was reported that small interfering RNA (siRNA)-mediated silencing of FXYD3 in Caco-2 cells inhibits Na,K-ATPase pump activity by decreasing its turnover (3). Therefore, we examined whether Na,K-ATPase activity is inhibited in FXYD3 knockdown Caco-2 cells by using a previously described method (43). As shown in Fig. 4E, membranes isolated from control Caco-2 cells exhibited Na,K-ATPase activity, whereas membranes isolated from FXYD3 knockdown cells did not ($P < 0.02$). Furthermore, the exposure of control membranes to recombinant ExoS also abrogated Na,K-ATPase activity ($P < 0.05$). These findings suggest that ExoS inactivates Na,K-ATPase activity through interactions with FXYD3.

ExoS alters tight junction components. We next studied whether the infection of Caco-2 cells with the wild-type strain influences the expression of the TJ-associated proteins occludin and ZO-1, which constitute the initial barrier to bacterial invasion. Western blot analysis revealed that infection of Caco-2 cells with the wild-type or Δ*exoS*/*exoS* strain reduced the levels of expression of ZO-1 (by 65 and 64%, respectively) and occludin (by 66 and 64%, respectively) relative to that observed following infection with the Δ*exoS* strain (Fig. 5A). In addition, confocal imaging revealed that infection of Caco-2 cells with the wild-type or Δ*exoS*/*exoS* strain disrupted TJ structure due to the reduced levels of expression of occludin and ZO-1 (Fig. 5B). These results are consistent with those of a previous study that reported that infection of polarized airway epithelial cells with *P. aeruginosa* expressing type III effectors (ExoS, ExoT, and ExoY) disrupts intact TJs by altering the distribution of the TJ proteins ZO-1 and occludin (44).

Immunoprecipitation of endogenous FXYD3 complexes. Endogenous FXYD3 complexes were precipitated by using an anti-FXYD3 antibody from lysates of Caco-2 cells infected with either PAO1 or the Δ*exoS* strain. ExoS was detected only in FXYD3 complexes precipitated from PAO1-infected Caco-2 cell lysates (Fig. 5C). Based on the results, we conclude

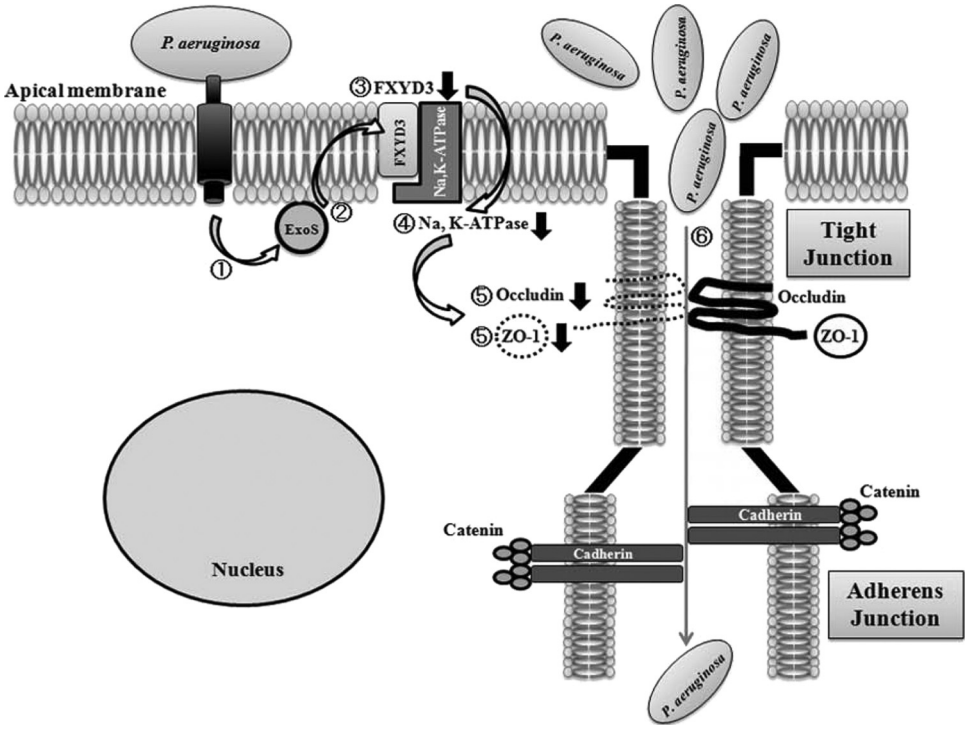

FIG. 6. Model for penetration of *P. aeruginosa* through the intestinal epithelial cell barrier on the basis of the interaction between ExoS and its binding partner FXYD3. The wild-type strain injects ExoS into the host epithelial cell (step 1), and ExoS migrates to the host cell membrane (step 2) and binds to FXYD3 (step 3). This binding of ExoS to FXYD3 inactivates FXYD3 (step 3) and subsequently reduces Na,K-ATPase activity (step 4). This inactivation of Na,K-ATPase inhibits the expression of the TJ proteins ZO-1 and occludin (step 5), leading to a disruption of the TJ structure, which allows *P. aeruginosa* to transmigrate effectively through the broken epithelial cell barrier (step 6).

that FXYD3 can bind ExoS both *in vivo* and *in vitro*. We next used confocal microscopy to document the colocalization of endogenous FXYD3 and ExoS in Caco-2 cells infected with PAO1 (Fig. 5D). As shown in Fig. 5D, the colocalization of endogenous FXYD3 and ExoS can be seen at Caco-2 cell membranes infected with PAO1, although there are nonspecific red-staining spots in Caco-2 cells infected with the Δ*exoS* strain and *E. coli*. On the basis of the results, we suggest that endogenous FXYD3 and ExoS may be colocalized in some areas of Caco-2 cells infected with PAO1.

DISCUSSION

In Fig. 6, we propose a model for bacterial penetration through the epithelial cell barrier on the basis of the interaction between ExoS and FXYD3. In this model, ExoS injected into the host epithelial cell migrates to the membrane (step 2), where it binds FXYD3 (step 3). The localization of ExoS after injection into mammalian cells has been investigated in detail previously (12, 20). Amino acid residues 51 to 72 of ExoS, which comprise a leucine-rich motif that forms a membrane localization domain, are required for localization to the plasma membrane. This membrane localization of ExoS is consistent with our model, whereby ExoS binds to FXYD3, since FXYD3 is localized to the apical membrane of polarized epithelial cells (13).

FXYD3 (Mat-8) regulates Na,K-ATPase and is expressed largely in the colon and stomach (10, 13). The colocalization of FXYD3 with Na,K-ATPase in Caco-2 cells was confirmed by the coimmunoprecipitation of FXYD3 with an Na,K-ATPase antibody (4). Bibert et al. previously reported that the silencing of FXYD3 in Caco-2 cells leads to a reduction in the TER and a decrease in maximal Na,K-ATPase activity owing to a decrease in its turnover (3). In the present study, we observed that the silencing of FXYD3 in Caco-2 cells leads to a slower increase in the TER and a reduction in Na,K-ATPase activity (Fig. 4C and E). Furthermore, we have also shown that exposure to recombinant ExoS can lead to a reduction in Na,K-ATPase activity (Fig. 4E). These results suggest that the binding of ExoS to FXYD3 causes an inactivation of FXYD3, followed by a reduction in Na,K-ATPase activity.

Na,K-ATPase is localized to the apical junction in mammalian epithelial cells, and the inhibition of Na,K-ATPase leads to an increase in tight junction permeability against ionic and nonionic solutes. These findings suggest that Na,K-ATPase activity is necessary for tight junction gate function (17, 42), although it was not clear whether Na,K-ATPase activity also regulated tight junction gate function against bacterial penetration. We have shown that the knockdown of FXYD3 leads to both a reduced activity of Na,K-ATPase and a disruption of tight junction gate function against bacterial penetration. FXYD3 thus appears to play a key role in forming the intact tight junction gate function against bacterial penetration by controlling Na,K-ATPase activity. *P. aeruginosa* ExoS targets FXYD3-regulated Na,K-ATPase activity in the apical membrane of epithelial cells to break the tight junction gate func-

tion and to achieve effective transmigration through the gate barrier. However, it is unclear how reduced Na,K-ATPase activity through the inactivation of FXYD3 disrupts tight junction gate function against bacterial penetration, and further studies will be needed.

We have developed a new model for the penetration of *P. aeruginosa* through the intestinal epithelial cell barrier (Fig. 6). These findings support the notion, based on epidemiological studies, that gut colonization with *P. aeruginosa* is a key pathogenic factor that underlies the development of invasive infections such as gut-derived sepsis. Since the expression of FXYD3 is known to be restricted to the colon and stomach, the prevention of the binding of ExoS to FXYD3 in the host intestine may be an effective way to interfere with *P. aeruginosa* translocation from the gut to the bloodstream, which may lead to the development of a new antibacterial agent to reduce the risk of gut-derived sepsis.

This penetration model for *P. aeruginosa* may be applicable to other pathogenic bacteria that employ secretion systems such as type III and type IV secretion systems to inject effector proteins into host cells. FXYD family proteins are widely distributed in mammalian tissues, although the expression of these proteins is tissue specific, and one of their common functions is interactions with Na,K-ATPase (4, 13, 16). Therefore, other pathogenic bacteria may use a similar strategy to penetrate the epithelial barrier in mammalian tissues by injecting effector proteins that can bind to FXYD family proteins.

Various bacterial functions are likely required for *P. aeruginosa* within the intestinal tract to reach and infect the bloodstream, including bacterial motility to reach epithelial cells, the ability to adhere to epithelial cells, the ability to penetrate the epithelial cell barrier, and resistance to phagocytic killing after invasion of the bloodstream. In the present study, we revealed that a type III effector, ExoS, plays an important role in bacterial penetration through the human intestinal epithelial cell barrier. However, this is one of the various steps necessary for *P. aeruginosa* to achieve gut-derived sepsis. A number of genes identified in our CGH analysis are known to encode virulence factors (data not shown). In addition, Hirakata et al. suggested previously that genes encoding multidrug efflux systems play an important role in the invasiveness of *P. aeruginosa* (24). Further studies will be required to clarify the contribution of these genes to *P. aeruginosa* virulence through the gut, which should eventually facilitate a more comprehensive understanding of the mechanism of bacterial translocation by *P. aeruginosa*.

ACKNOWLEDGMENTS

We thank H. Ito and T. Niga for CGH analysis, H. Hamamoto and K. Sekimizu for advice on silkworm experiments, and Y. Hirakata for supporting penetration assays.

REFERENCES

1. **Alverdy, J., C. Holbrook, F. Rocha, L. Seiden, R. L. Wu, M. Musch, E. Chang, D. Ohman, and S. Suh.** 2000. Gut-derived sepsis occurs when the right pathogen with the right virulence genes meets the right host: evidence for in vivo virulence expression in *Pseudomonas aeruginosa*. Ann. Surg. **232:**480–489.
2. **Bertrand, X., M. Thouverez, D. Talon, A. Boillot, G. Capellier, C. Floriot, and J. P. Hélias.** 2001. Endemicity, molecular diversity and colonisation routes of *Pseudomonas aeruginosa* in intensive care units. Intensive Care Med. **27:**1263–1268.
3. **Bibert, S., D. Aebischer, F. Desgranges, S. Roy, D. Schaer, S. Kharoubi-Hess, J. D. Horisberger, and K. Geering.** 2009. A link between FXYD3 (Mat-8)-mediated Na,K-ATPase regulation and differentiation of Caco-2 intestinal epithelial cells. Mol. Biol. Cell **20:**1132–1140.
4. **Bibert, S., S. Roy, D. Schaer, E. Felley-Bosco, and K. Geering.** 2006. Structural and functional properties of two human FXYD3 (Mat-8) isoforms. J. Biol. Chem. **281:**39142–39151.
5. **Blair, P., B. J. Rowlands, K. Lowry, H. Webb, P. Armstrong, and J. Smilie.** 1991. Selective decontamination of the digestive tract: a stratified, randomized, prospective study in a mixed intensive care unit. Surgery **110:**303–309.
6. **Boman, H. G., I. Nilsson, and B. Rasmuson.** 1972. Inducible antibacterial defence system in *Drosophila*. Nature **237:**232–235.
7. **Chen, Y., Q. Lu, E. E. Schneeberger, and D. A. Goodenough.** 2000. Restoration of tight junction structure and barrier function by down-regulation of the mitogen-activated protein kinase pathway in ras-transformed Madin-Darby canine kidney cells. Mol. Biol. Cell **11:**849–862.
8. **Coburn, J., and D. M. Gill.** 1991. ADP-ribosylation of p21ras and related proteins by *Pseudomonas aeruginosa* exoenzyme S. Infect. Immun. **59:**4259–4262.
9. **Coburn, J., R. T. Wyatt, B. H. Iglewski, and D. M. Gill.** 1989. Several GTP-binding proteins, including p21c-H-ras, are preferred substrates of *Pseudomonas aeruginosa* exoenzyme S. J. Biol. Chem. **264:**9004–9008.
10. **Crambert, G., C. Li, D. Claeys, and K. Geering.** 2005. FXYD3 (Mat-8), a new regulator of Na,K-ATPase. Mol. Biol. Cell **16:**2363–2371.
11. **de Jonge, E., M. J. Schultz, L. Spanjaard, P. M. Bossuyt, M. B. Vroom, J. Dankert, and J. Kesecioglu.** 2003. Effects of selective decontamination of digestive tract on mortality and acquisition of resistant bacteria in intensive care: a randomised controlled trial. Lancet **362:**1011–1016.
12. **Deng, Q., Y. Zhang, and J. T. Barbieri.** 2007. Intracellular trafficking of *Pseudomonas* ExoS, a type III cytotoxin. Traffic **8:**1331–1345.
13. **Franzin, C. M., X. Gong, P. Teriete, and F. M. Marassi.** 2007. Structures of the FXYD regulatory proteins in lipid micelles and membranes. J. Bioenerg. Biomembr. **39:**379–383.
14. **Franzin, C. M., P. Teriete, and F. M. Marassi.** 2007. Structural similarity of a membrane protein in micelles and membranes. J. Am. Chem. Soc. **129:**8078–8079.
15. **Furuya, N., Y. Hirakata, K. Tomono, T. Matsumoto, K. Tateda, M. Kaku, and K. Yamaguchi.** 1993. Mortality rates amongst mice with endogenous septicaemia caused by *Pseudomonas aeruginosa* isolates from various clinical sources. J. Med. Microbiol. **39:**141–146.
16. **Geering, K.** 2006. FXYD proteins: new regulators of Na-K-ATPase. Am. J. Physiol. Renal Physiol. **290:**F241–F250.
17. **Geering, K.** 2008. Functional roles of Na,K-ATPase subunits. Curr. Opin. Nephrol. Hypertens. **17:**526–532.
18. **Goehring, U. M., G. Schmidt, K. J. Pederson, K. Aktories, and J. T. Barbieri.** 1999. The N-terminal domain of *Pseudomonas aeruginosa* exoenzyme S is a GTPase-activating protein for Rho GTPases. J. Biol. Chem. **274:**36369–36372.
19. **Hamamoto, H., K. Kamura, I. M. Razanajatovo, K. Murakami, T. Santa, and K. Sekimizu.** 2005. Effects of molecular mass and hydrophobicity on transport rates through non-specific pathways of the silkworm larva midgut. Int. J. Antimicrob. Agents **26:**38–42.
20. **Hauser, A. R.** 2009. The type III secretion system of *Pseudomonas aeruginosa*: infection by injection. Nat. Rev. Microbiol. **7:**654–665.
21. **Heeb, S., B. Caroline, and H. Dieter.** 2002. Regulatory RNA as mediator in GacA/RsmA-dependent global control of exoproduct formation in *Pseudomonas fluorescens* CHA0. J. Bacteriol. **184:**1046–1056.
22. **Henriksson, M. L., M. S. Francis, A. Peden, M. Aili, K. Stefansson, R. Palmer, A. Aitken, and B. Hallberg.** 2002. A nonphosphorylated 14-3-3 binding motif on exoenzyme S that is functional in vivo. Eur. J. Biochem. **269:**4921–4929.
23. **Henriksson, M. L., C. Sundin, A. L. Jansson, A. Forsberg, R. H. Palmer, and B. Hallberg.** 2002. Exoenzyme S shows selective ADP-ribosylation and GTPase-activating protein (GAP) activities towards small GTPases in vivo. Biochem. J. **367**(Pt. 3)**:**617–628.
24. **Hirakata, Y., R. Srikumar, K. Poole, N. Gotoh, T. Suematsu, S. Kohno, S. Kamihira, R. E. Hancock, and D. P. Speert.** 2002. Multidrug efflux systems play an important role in the invasiveness of *Pseudomonas aeruginosa*. J. Exp. Med. **196:**109–118.
25. **Hoang, T. T., R. R. K. Schweize, A. J. Kutchma, and H. P. Schweizer.** 1998. A broad-host-range Flp-*FRT* recombination system for site-specific excision of chromosomally-located DNA sequences: application for isolation of unmarked *Pseudomonas aeruginosa* mutants. Gene **212:**77–86.
26. **Hossain, M. S., H. Hamamoto, Y. Matsumoto, I. M. Razanajatovo, J. Larranaga, C. Kaito, H. Kasuga, and K. Sekimizu.** 2006. Use of silkworm larvae to study pathogenic bacterial toxins. J. Biochem. **140:**439–444.
27. **Jander, G., L. G. Rahme, and F. M. Ausubel.** 2000. Positive correlation between virulence of *Pseudomonas aeruginosa* mutants in mice and insects. J. Bacteriol. **182:**3843–3845.
28. **Kaito, C., K. Kurokawa, Y. Matsumoto, Y. Terao, S. Kawabata, S. Hamada, and K. Sekimizu.** 2005. Silkworm pathogenic bacteria infection model for identification of novel virulence genes. Mol. Microbiol. **56:**934–944.
29. **Kovach, M. E., P. H. Elzer, D. S. Hill, G. T. Robertson, M. A. Farris, R. M. Roop, and K. M. Peterson.** 1995. Four new derivatives of the broad-host-

range cloning vector pBBR1MCS carrying different antibiotic-resistance cassettes. Gene **166:**175–176.
30. **Kuwayama, H., S. Obara, T. Morio, M. Katoh, H. Urushihara, and Y. Tanaka.** 2002. PCR mediated generation of a gene disruption construct without the use of DNA ligase and plasmid vectors. Nucleic Acids Res. **30:**E2.
31. **Ledingham, I. M., S. R. Alcock, A. T. Eastaway, J. C. McDonald, I. C. McKay, and G. Ramsay.** 1988. Triple regimen of selective decontamination of the digestive tract, systemic cefotaxime, and microbiological surveillance for prevention of acquired infection in intensive care. Lancet **i:**785–790.
32. **Lutter, E. I., M. M. Faria, H. R. Rabin, and D. G. Storey.** 2008. *Pseudomonas aeruginosa* cystic fibrosis isolates from individual patients demonstrate a range of levels of lethality in two *Drosophila melanogaster* infection models. Infect. Immun. **76:**1877–1888.
33. **Mahajan-Miklos, S., M. W. Tan, L. G. Rahme, and F. M. Ausubel.** 1999. Molecular mechanisms of bacterial virulence elucidated using a *Pseudomonas aeruginosa-Caenorhabditis elegans* pathogenesis model. Cell **96:**47–56.
34. **Marshall, J. C., N. V. Christou, and J. L. Meakins.** 1993. The gastrointestinal tract. The "undrained abscess" of multiple organ failure. Ann. Surg. **218:** 111–119.
35. **Matsumoto, T., N. Furuya, K. Tateda, S. Miyazaki, A. Ohno, Y. Ishii, Y. Hirakata, and K. Yamaguchi.** 1999. Effect of passive immunotherapy on murine gut-derived sepsis caused by *Pseudomonas aeruginosa*. J. Med. Microbiol. **48:**765–770.
36. **Matsumoto, T., K. Tateda, S. Miyazaki, N. Furuya, A. Ohno, Y. Ishii, Y. Hirakata, and K. Yamaguchi.** 1997. Adverse effects of tumour necrosis factor in cyclophosphamide-treated mice subjected to gut-derived *Pseudomonas aeruginosa* sepsis. Cytokine **9:**763–769.
37. **Matsumoto, T., K. Tateda, S. Miyazaki, N. Furuya, A. Ohno, Y. Ishii, Y. Hirakata, and K. Yamaguchi.** 1998. Effect of interleukin-10 on gut-derived sepsis caused by *Pseudomonas aeruginosa* in mice. Antimicrob. Agents Chemother. **42:**2853–2857.
38. **Matsumoto, T., K. Tateda, S. Miyazaki, N. Furuya, A. Ohno, Y. Ishii, Y. Hirakata, and K. Yamaguchi.** 1997. Immunomodulating effect of fosfomycin on gut-derived sepsis caused by *Pseudomonas aeruginosa* in mice. Antimicrob. Agents Chemother. **41:**308–313.
39. **Miyauchi, E., H. Morita, J. Okuda, T. Sashihara, M. Shimizu, and S. Tanabe.** 2008. Cell wall fraction of *Enterococcus hirae* ameliorates TNF-alpha-induced barrier impairment in the human epithelial tight junction. Lett. Appl. Microbiol. **46:**469–476.
40. **Okuda, J., T. Toyotome, N. Kataoka, M. Ohno, H. Abe, Y. Shimura, A. Seyedarabi, R. Pickersgill, and C. Sasakawa.** 2005. *Shigella* effector IpaH9.8 binds to a splicing factor U2AF(35) to modulate host immune responses. Biochem. Biophys. Res. Commun. **333:**531–539.
41. **Osmon, S., S. Ward, V. J. Fraser, and M. H. Kollef.** 2004. Hospital mortality for patients with bacteremia due to *Staphylococcus aureus* or *Pseudomonas aeruginosa*. Chest **125:**607–616.
42. **Rajasekaran, S. A., S. P. Barwe, J. Gopal, S. Ryazantsev, E. E. Schneeberger, and A. K. Rajasekaran.** 2007. Na-K-ATPase regulates tight junction permeability through occludin phosphorylation in pancreatic epithelial cells. Am. J. Physiol. Gastrointest. Liver Physiol. **292:**G124–G133.
43. **Sarkar, P. K.** 2002. A quick assay for Na^+-K^+-ATPase specific activity. Z. Naturforsch. C **57:**562–564.
44. **Soong, G., D. Parker, M. Magargee, and A. S. Prince.** 2008. The type III toxins of *Pseudomonas aeruginosa* disrupt epithelial barrier function. J. Bacteriol. **190:**2814–2821.
45. **Stirling, F. R., and T. J. Evans.** 2006. Effects of the type III secreted pseudomonal toxin ExoS in the yeast *Saccharomyces cerevisiae*. Microbiology **152:**2273–2285.
46. **Stoutenbeek, C. P., H. K. van Saene, D. R. Miranda, and D. F. Zandstra.** 1984. The effect of selective decontamination of the digestive tract on colonisation and infection rate in multiple trauma patients. Intensive Care Med. **10:**185–192.
47. **Vikström, E., L. Bui, P. Konradsson, and K. E. Magnusson.** 2009. The junctional integrity of epithelial cells is modulated by *Pseudomonas aeruginosa* quorum sensing molecule through phosphorylation-dependent mechanisms. Exp. Cell Res. **315:**313–326.
48. **Watanabe, R., T. Matsumoto, G. Sano, Y. Ishii, K. Tateda, Y. Sumiyama, J. Uchiyama, S. Sakurai, S. Matsuzaki, S. Imai, and K. Yamaguchi.** 2007. Efficacy of bacteriophage therapy against gut-derived sepsis caused by *Pseudomonas aeruginosa* in mice. Antimicrob. Agents Chemother. **51:**446–452.
49. **Würtele, M., L. Renault, J. T. Barbieri, A. Wittinghofer, and E. Wolf.** 2001. Structure of the ExoS GTPase activating domain. FEBS Lett. **491:**26–29.
50. **Yamamoto, H., K. Okumura, S. Toshima, K. Mukaisho, H. Sugihara, T. Hattori, M. Kato, and S. Asano.** 2009. FXYD3 protein involved in tumor cell proliferation is overproduced in human breast cancer tissues. Biol. Pharm. Bull. **32:**1148–1154.
51. **Zaborina, O., J. E. Kohler, Y. Wang, C. Bethel, O. Shevchenko, L. Wu, J. R. Turner, and J. C. Alverdy.** 2006. Identification of multi-drug resistant *Pseudomonas aeruginosa* clinical isolates that are highly disruptive to the intestinal epithelial barrier. Ann. Clin. Microbiol. Antimicrob. **5:**14.

Editor: B. A. McCormick